Oxygen dynamics at the base of a biofilm studied with planar optodes

Ronnie Nøhr Glud[1,2,*], Cecilia Maria Santegoeds[1], Dirk De Beer[1], Oliver Kohls[1], Niels Birger Ramsing[3]

[1]Max Planck Institute for Marine Microbiology, Celsiusstr. 1, D-28359 Bremen, Germany
[2]University of Copenhagen, Marine Biological Laboratory, Strandpromenaden 5, DK-3000 Helsingør, Denmark
[3]University of Aarhus, Institute of Biology, Dept of Microbial Ecology, Ny Munkegade bgn. 550, DK-8000 Århus C, Denmark

ABSTRACT: The O_2 dynamics at the base of biofilms was studied using planar optodes. Biofilms were grown directly on the optodes and the 2-dimensional distribution of O_2 at the base of biofilms was resolved at a spatial resolution of 30×30 µm, using a CCD camera. The average O_2 saturation at the base decreased and the heterogeneity increased as biofilms developed. In mature biofilms heterogeneous O_2 distributions were caused by clusters of high biomass which had low O_2 saturations surrounded by O_2-rich voids and channels. The O_2 distribution at the base of biofilms was highly dependent on the free flow velocity above the biofilm, e.g. in a 400 µm thick biofilm the average O_2 saturation increased from 0 to 23.1% air saturation as the free flow velocity increased from 6.2 to 35.1 cm s^{-1} Addition of glucose to a concentration of 2 mM in the water phase at maximum flow velocity caused the O_2 consumption rate to increase and the base of the biofilm to go anoxic. The insertion of an O_2 microelectrode into a biofilm caused the O_2 saturation at the base of the biofilm to increase by approximately 25 µM. This effect, presumably caused by hydrodynamic disturbances, typically extended several mm away from the position of the microsensor tip. The presented data show for the first time the true distribution of O_2 at the basis of heterogeneous biofilms and demonstrate the great potential of planar optodes for the study of solute dynamics within biofilms at a very high spatial and temporal resolution.

KEY WORDS: Optodes · Flow · Microniches

INTRODUCTION

Under physiological conditions most submerged surfaces will become colonized by bacteria that gradually form denser biofilms. During the initial development, the base of a biofilm will be all oxic; however, as the thickness increases anoxic areas are expected to occur. The metabolism and function of such communities are largely controlled by the electron acceptors available above and within the biofilm. Oxygen is energetically the most favorable electron acceptor and it therefore plays an important role for the turnover of organic matter within a biofilm. Further, O_2 acts as a reoxidizer

of reduced compounds diffusing up to the oxic zone from deeper layers. The oxic conditions within a biofilm also determine the extent to which denitrification is coupled to nitrification and consequently regulate how well a biofilm acts as a NO_3^- scavenger (Dalsgaard & Revsbech 1992).

Biofilms may not be homogeneous layers of cells, as conventionally thought, but often have a complex heterogeneous structure that is dependent on growth conditions and the microbial composition (e.g. Lawrence et al. 1991, Caldwell et al. 1992). Recent investigations with confocal microscopy have shown that they typically contain dense cell clusters, surrounded by voids (Costerton et al. 1994, De Beer et al. 1994a). Liquid may flow through the voids, insuring an efficient exchange of solutes between the biofilm and the water

*E-mail: mblrg@mail.centrum.dk

phase, and probably enables cells to maintain a high growth rate. The patchy distribution of reduced and oxidized zones in well-developed biofilms may initiate pit corrosion on metal surfaces, and the O_2 distribution is of importance for metal corrosion in aquatic environments (Ford & Mitchell 1991). To resolve the heterogeneous distribution and dynamics of solutes like O_2 within such a community, techniques with a high spatial and temporal resolution are required (De Beer et al. 1994b).

Due to their small size, high spatial resolution, fast response time and low stirring sensitivity, microelectrodes are ideal tools for studying O_2 dynamics in compact, laminated benthic communities (Revsbech & Jørgensen 1986, Glud et al. 1992, Canfield & Des Marais 1993). Recently, a new fiber optic microsensor (microoptode), which complements the microelectrode, has been developed and applied in the field of aquatic biology (Klimant et al. 1995). The main advantages of optodes include a better long-term stability and simpler manufacturing procedures as compared to O_2 microelectrodes. The measuring principle in this sensor is based on the dynamic quenching of an immobilized fluorophore by O_2, which decreases the fluorescence quantum yield (Kautsky 1939). In microoptodes, the fluorophore is fixed to the tip of a beveled glass fiber and the excitation light is guided through the fiber to the tip of the sensor. The fiber also guides the fluorescent light emitted by the fluorophore after excitation back to the measuring circuit (Klimant et al. 1995).

Both types of microsensors measure the O_2 tension at a single point and microprofiles are obtained by moving the sensor stepwise within the medium. However, in the spatially heterogeneous biofilms described above, a large number of profiles are required in order to describe the solute dynamics. Further, it has been shown that the presence of a microsensor can change the distribution of O_2 within sediments due to a hydrodynamic disturbance of the diffusive boundary layer (DBL); such effects must be expected to be more pronounced in biofilms with steep concentration gradients (Glud et al. 1994). In other words, to quantify and describe the O_2 dynamics within a heterogeneous biofilm, non-conventional techniques are required. Techniques combining color indicators for specific solutes with microscopy and digital imaging have been attempted; however, calibration problems related to determination of the indicator concentration have often hampered the use of these techniques (Caldwell et al. 1992).

Recently an alternative approach based on the principle of dynamic quenching, planar optodes, has allowed 2-dimensional determination of O_2 dynamics within marine sediments (Glud et al. 1996). Instead of fixing an immobilized fluorophore to the tip of a microoptode, the sensing agent was immobilized in thin sheets, 'planar optodes'. Images of the O_2-sensitive fluorescent light emitted by the planar optode were acquired with a CCD camera, allowing quantification of the O_2 saturation in front of the planar optode (Glud et al. 1996). The optodes are simple to construct and a robust calibration routine ensures high quality data. By growing biofilms directly on planar optodes we were able to quantify the 2-dimensional O_2 dynamics at the base of a biofilm without disturbance. We hereby present data that quantify O_2 saturations and dynamics at the base of biofilms as a function of the biofilm development (thickness), flow velocity of the overlying water, and addition of organic substrates.

MATERIALS AND METHODS

Planar oxygen optode. The planar optodes consisted of 3 layers: a transparent polyester support foil 175 µm thick, a 10 µm sensing layer and a 20 µm black silicone layer (Glud et al. 1996). The polyester support foil was included in order to handle and fix the sensing agent in the experimental setup described below. The sensing layer consisted of an immobilized O_2 quenchable ruthenium complex, which had maximum light absorbance in the blue range and emitted red fluorescent light (Klimant & Wolfbeis 1995). In order to increase the scatter intensity, titanium dioxide grains (diameter approximately 1 µm) were added (Klimant & Wolfbeis 1995). The black silicone acted as an optical isolation, which insured that the excitation light never reached the internal parts of the experimental setup and that scatter in the biofilms did not affect the CCD images (for more details see Glud et al. 1996). The size of the employed planar optodes was 25×55 mm.

Experimental setup. All experiments were performed in a 100 cm long and 4 cm wide transparent flow cell. An adjustable circulation micropump (Ismatec, MC-Z) insured a stable but adjustable flow rate above the biofilm (Fig. 1A). Medium was added to the flow cell through a peristaltic pump (Gilson M312), and a constant overflow maintained the water level and nutrient concentration for a given flow velocity (Fig. 1A). The minimal medium was added at a rate of 50 ml min^{-1} and consisted of KH_2PO_4 (220 µM), K_2HPO_4 (400 µM), $(NH_4)_2SO_4$ (760 µM), Na-acetate (200 µM) and $MgSO_4$ (41 µM). A Clark type O_2 microelectrode (tip size <5 µm) was used to continuously monitor the O_2 saturation in the free flowing water phase (Revsbech & Jørgensen 1986, Revsbech 1989).

The planar optode was fixed to the bottom of the dry flow cell by a thin film of transparent silicone and thereafter it cured for 24 h. The planar optode was excited by a halogen lamp equipped with a bandpass

glass filter (BG 12, Schott, Germany) in order to eliminate yellow and red light from the excitation beam (Fig. 1B). A CCD Photometrics™ camera (CH250L) equipped with a 60 mm Nikon macro lens and a long-pass glass filter (OG 570, Schott) was positioned below the flow cell at a distance of approximately 15 cm (Fig. 1B). The flow cell, the halogen lamp, and the CCD camera were fixed relative to each other in a custom designed frame, in order to minimize vibration effects. The flow cell was inoculated by 10 ml activated sludge from a waste water treatment plant, and after 10 to 12 d an approximately 400 µm thick biofilm covered the bottom of the flow cell and the planar optode. Images were obtained by the CCD camera as a function of time (biofilm development), free flow velocity of the overlying water and concentrations of organic substances in the overlying water.

After each series of experiments the biofilm covering the investigated part of the planar optode was removed for calibration purposes. Images were obtained at 3 to 5 different O_2 saturations. The saturation was adjusted by flushing with N_2 gas in the overflow bottle and was measured by the calibrated O_2 microelectrode (Fig. 1A). A stereo microscope allowed visual inspection of the biofilm and capillaries inserted by a micromanipulator were used to measure the thickness of the biofilms. All experiments were performed in a darkened thermostat room at 20°C.

Image recording, calibration and analysis. The camera was equipped with a Peltier cooled CCD chip (KAF 1400, 1317 × 1035 pixels, 6.8 × 6.8 µm) and was controlled by a Macintosh Quadra computer. The images were obtained using an aperture of 2.8 and an exposure time of 0.01 s. The digital pictures were acquired as 12 bit grey-scale images with the program NU-200, Photometrics, and stored in a 16 bit TIFF format for later analysis. In order to reduce the time required for calculations, the images were obtained with a binning factor of 2, implying that only an average value for each set of 4 neighboring pixels was stored. This reduced the original number of pixels to 3.4 × 10⁵, the images covered 19.7 × 15.6 mm and consequently the spatial resolution in both directions was about 30 µm. The investigated area and the spatial resolution of the obtained images could be adjusted by applying lenses of different focal length.
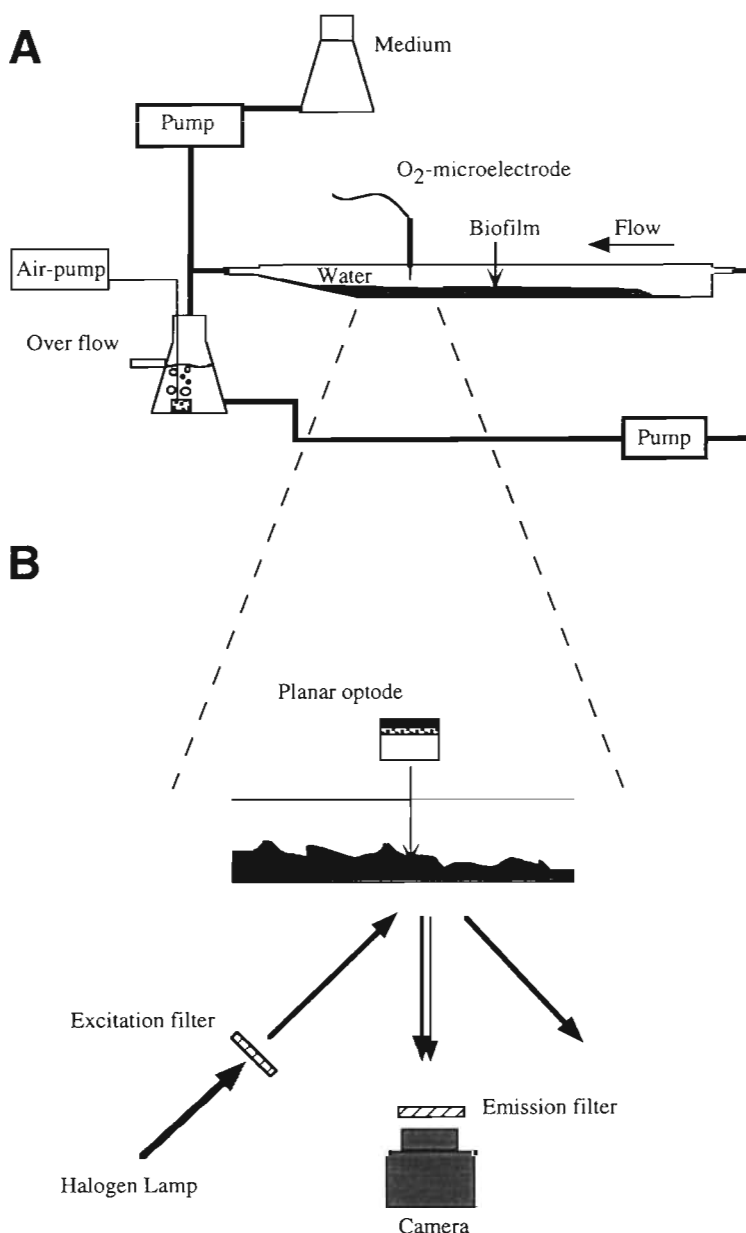

Fig. 1. Schematic drawing of the experimental setup. (B) Enlargement of the area around the planar optode including camera, filters, etc., which is omitted in (A). For details see text

For most optodes the emitted light intensity (I) can be approached by a modified Stern-Volmer equation (Klimant et al. 1995):

$$I = I_0\left[\alpha + (1-\alpha)\left(\frac{1}{1 + K_{SV}C}\right)\right] \quad (1)$$

where α is the non-quenchable fraction of the fluorescence, I_0 is the fluorescence intensity in the absence of O_2, K_{SV} is the quenching constant and C is the O_2

saturation. Due to the relatively heterogeneous planar optodes used in our experiments, each of these parameters was found to be pixel dependent (Glud et al. 1996). Consequently we had to perform 3 point calibration of each individual pixel. To do so, we used the calibration images obtained after each experiment. The I_0 value of each pixel was determined directly from an image obtained with no O_2 in the overlying water, while the pixel values of α and K_{SV} were calculated based on the 2 additional calibration images. The necessary equations are derived in Glud et al. (1996). Knowing all 3 calibration constants, the pixel dependent O_2 saturation in the acquired images could be derived from Eq. (2):

$$C = \frac{I_0 - I}{K_{SV}(I - I_0\alpha)} \qquad (2)$$

After appropriate calibration the O_2 saturation was depicted on a 8 bit color scale (256 different colors), with a chosen max/min O_2 value.

RESULTS

Biofilm development

After inoculation, the free flow velocity in the flow cell was kept at an intermediary level of approximately 25 cm s^{-1}. A thin opaque layer of polysaccharides soon covered the planar optode, as observed through a stereo microscope. Gradually, flocculent material embedded in the opaque layer and grew into a heterogeneous biofilm. The inoculation was repeated 3 times and every time it took between 10 and 12 d for a biofilm with an average thickness of 400 µm to develop. The surface of the biofilm was characterized by an extensive variation in microtopography and generally developed faster further downstream in the flow cell. As the biofilm grew in thickness the average O_2 saturation at the base of the biofilm decreased correspondingly (Fig. 2). For the interpretation of Fig. 2 it is important to notice that the measurements were made
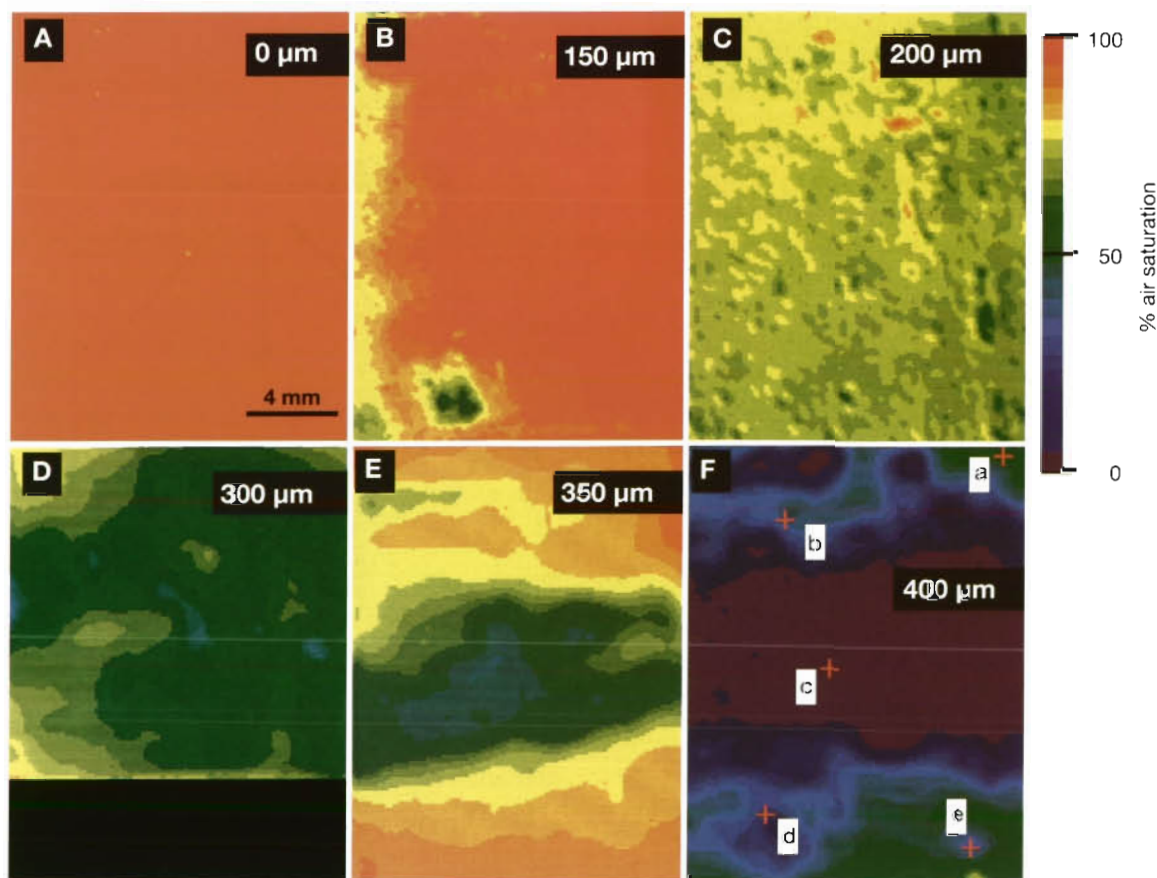

Fig. 2. O_2 saturation at the base of 6 different biofilms, (A) 0 d, (B) 4 d, (C) 8 d and (D–F) 11 to 13 d after inoculation (average thickness indicated). For clarification the original 8 bit color scale is reduced to 26 colors. The flow direction was in all instances from right to left and the velocity approximately 20 cm s^{-1}. The black box in (D) covers an area of the planar optode that was obscured by the reflection from a screw in the bottom of the flow cell. The 5 points indicated in (F) were used in the experiments with changed flow velocities (Figs. 3 & 5). A scale bar is shown in (A)

on different biofilms and it is therefore not possible to follow the same area during different development stages. The initial measurement just after inoculation resulted in a homogenous signal that corresponded to 100 % air saturation (284 µM) (Fig. 2A). After 4 d a thin biofilm covered the optode, but most of the sensor still experienced full air saturation (Fig. 2B). However, at the very left, the biofilm was thicker and the average O_2 saturation at the base of this area was 80.3 % (227 µM), while single aggregates resulted in O_2 saturation down to 57.0 % (162 µM) (Fig. 2B). After 8 d the planar optode was covered by a 200 µm (on average) thin biofilm and the average O_2 saturation at the base had decreased to 64.1 % (182 µM) (Fig. 2C). Fig. 2D–F represents 3 different biofilms 11 to 13 d after inoculation. In Fig. 2D the average O_2 saturation had further decreased to 52.3 % (149 µM) and areas with O_2 saturations below 20 % (57 µM) were apparent. In Fig. 2E the saturation varied extensively: the central area had an O_2 saturation below 20.0 % (57 µM) whereas the surrounding areas had higher O_2 tensions approaching air saturation. The central area of the biofilm which had developed to an average thickness of 400 µm was anoxic at the base (Fig. 2F) and, as for the biofilm presented in Fig. 2E, horizontal O_2 gradients from the center to the periphery of the image had evolved.

Flow effects on the O_2 distribution at the base of a biofilm

The O_2 saturation at the base of the 12 d old biofilm presented in Fig. 2F was measured after the free flow velocity of the overlying water was reduced from 35.1 to 6.2 cm s^{-1}. After changing the flow velocity, the average O_2 saturation started to decrease and the base of the biofilm reached complete anoxia 6 min later (Fig. 3A). The average O_2 decrease followed a sigmoidal curve with a maximum rate of decrease after 1.5 min. However, different pixels responded very differently, probably caused by differences in local biofilm thickness, transport coefficients and respiration rates (Fig. 3B).

One day later the steady state O_2 saturation at the base of the same biofilm was measured at different flow velocities of the overlying water; 6 examples are presented in Fig. 4. The average O_2 saturation increased from 0 to 23.1 % (0 to 66 µM) when the free flow velocity was increased from 6.2 to 35.1 cm s^{-1} (Fig. 5A). However, it is apparent from Fig. 4 that some areas in the biofilm were more sensitive to flow than others. At 20.5 cm s^{-1}, areas with increased O_2 saturations had developed in the otherwise anoxic surroundings and as the flow increased these areas gradually grew and became connected (Fig. 4). At the highest flow velocities, numerous 'islands', with low O_2 satura-
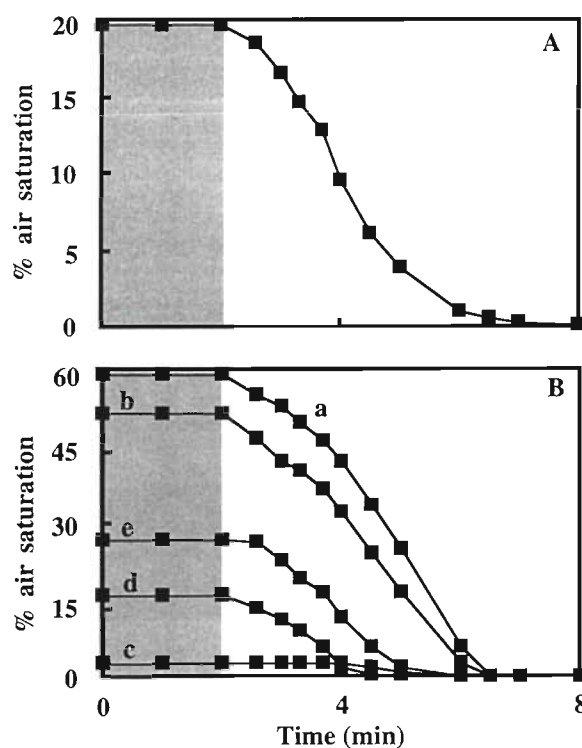

Fig. 3. (A) Average % air saturation at the base of a 12 d old biofilm as the flow velocity of the overlying water was changed from 35.1 (gray shaded) to 6.2 cm s^{-1}. (B) Corresponding data for the 5 individual positions indicated in Fig. 2F

tions in otherwise O_2-rich surroundings, still remained (Fig. 4F). These islands exhibited steeper O_2 gradients in the direction against the flow as compared to the 'lee' side of the islands. Even at the maximum flow rate no pixels reached full saturation (Fig. 4F). By decreasing the flow velocity in steps, the O_2 conditions prior to increased flow conditions could be re-established, indicating that the biofilm did not change physically during the increased flow scenario (data not shown).

The observations that different areas of the biofilm responded differently to flow increases are emphasized in Figs. 5B & 6. Fig. 5B shows the O_2 saturation for 6 different pixels (indicated in Fig. 4A) at different flow regimes. The O_2 saturation at pixel c only changed marginally as the flow was increased from 10.9 to 20.5 cm s^{-1} and pixel d and f were almost insensitive to the flow until it exceeded 23.4 cm s^{-1}. Here the O_2 saturation increased, but then remained at a constant level; this was also found for pixel e until the flow reached 33.1 cm s^{-1}. The O_2 saturation at pixels b and a increased almost linearly with flow and at maximum flow velocity it reached 49.1 % (139 µM) and 61.7 % air saturation (175 µM), respectively.

Pixel values along a line perpendicular to the flow direction (indicated in Fig. 4A) are presented as a
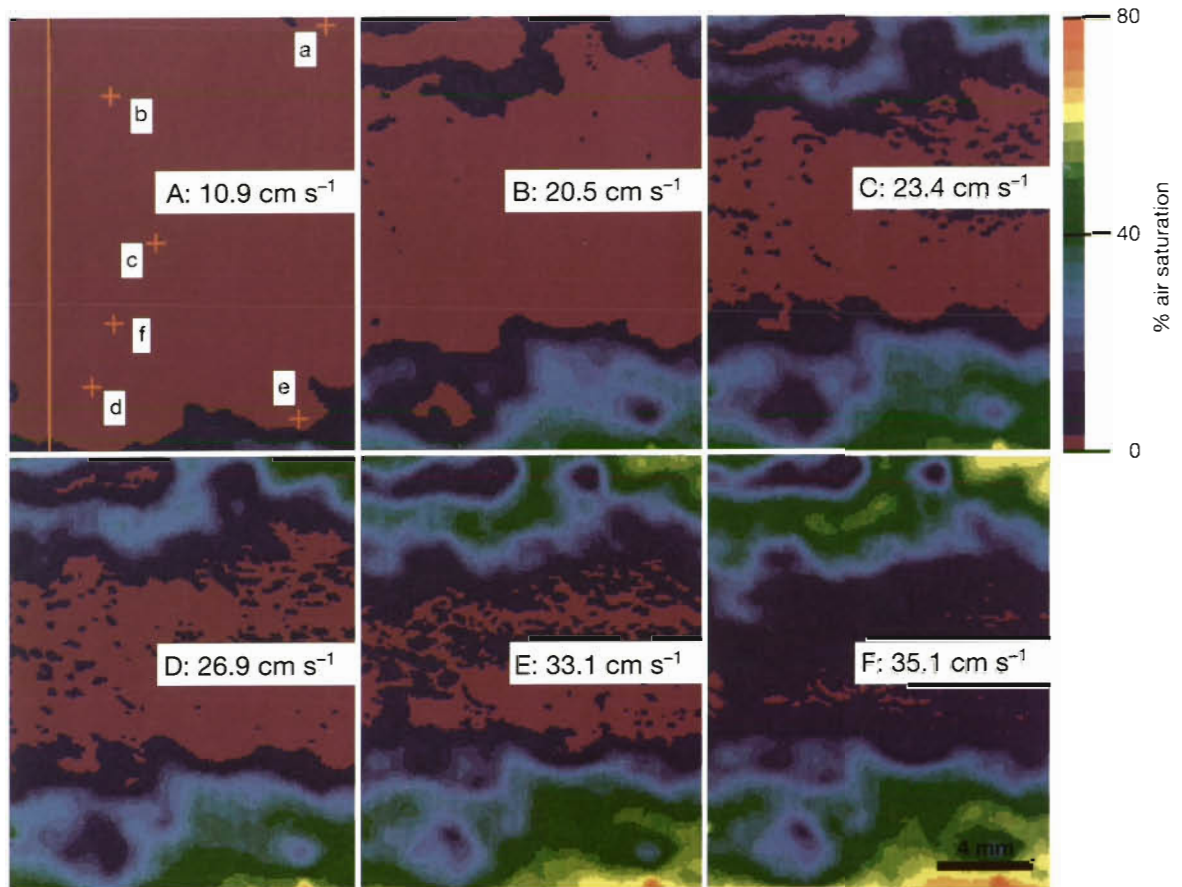
Fig. 4. Oxygen images of the base of a 13 d old biofilm at increasing flow velocities. Positions investigated in greater details in Figs. 5B & 6 are in (A). A scale bar for the dimensions is indicated in (F) and the flow direction was from right to left

function of flow in Fig. 6. The positions of local maxima and minima appeared flow-insensitive, as expected if they corresponded to metabolic hot spots. The O_2 gradients between them were likewise in many cases flow-insensitive. It is apparent that whole areas exhibited the same stepwise response to flow changes, as e.g. pixels d, e and f, in Fig. 5B; pixels between 14 and 19.5 mm were almost insensitive to the flow increases from 23.4 to 26.9 and 33.1 to 35.1 cm s^{-1}, while the pix-

els between 3 and 5 mm clearly showed increased O_2 saturations at the same flow increases. At the highest flow velocity, no positions were anoxic and notably positions from 6 to 8 mm showed a dramatic increase in O_2 saturation during the last flow increase. During all flow experiments the overlying water was fully air saturated. Repeating the flow experiments with the biofilms presented in Fig. 2D & E resulted in similar observations.
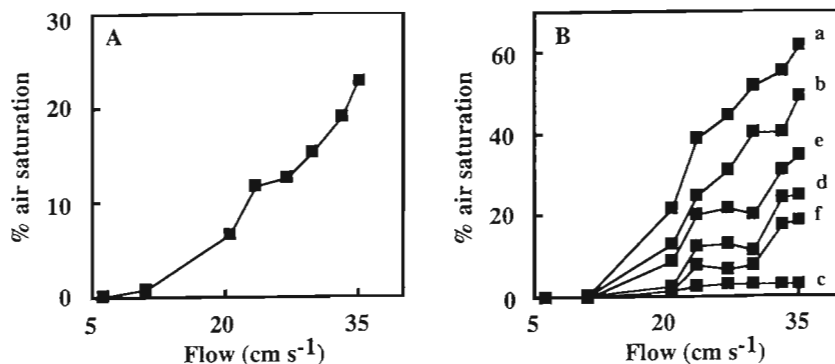

Fig. 5. (A) Average O_2 saturation at the base of a 13 d old biofilm as a function of the flow velocity of the overlying water. (B) Equivalent values for individual pixels indicated in Fig. 4A
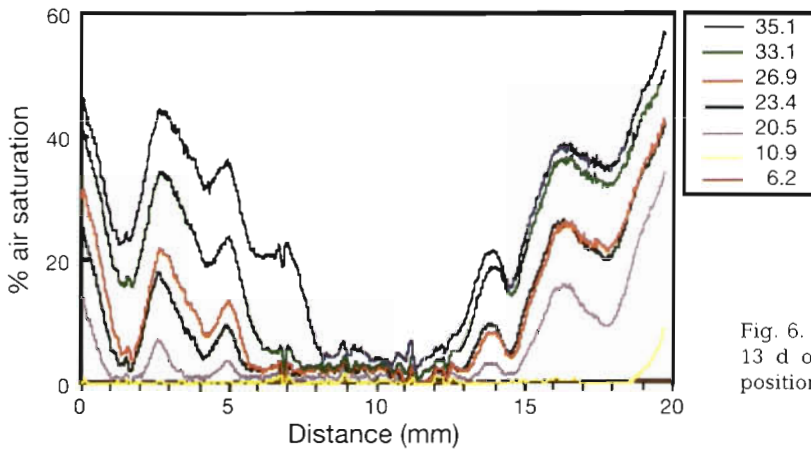
Fig. 6. O_2 saturation along a transect at the base of a 13 d old biofilm at 7 different flow velocities. The position of the transect is indicated by a line in Fig. 4A, where 0 indicates the upper corner

Oxygen images were acquired as a microelectrode in the overlying water was inserted into the biofilm (Fig. 7). Below the sensor tip, the O_2 saturation gradually increased as the O_2 microsensor was moved downward. When the sensor was 200 µm above the surface of the biofilm the O_2 saturation had increased by 6.3% air saturation (18 µM) below the sensor tip, and the value further increased to 9.1% (26 µM) as the sensor was inserted into the biofilm (Fig. 7A–C). The horizontal distribution of the disturbance extended approximately 3 mm perpendicular to the flow direction and more than 5 mm downstream from the sensor tip. After removal of the microelectrode, the original O_2 conditions were re-established. The experiment was repeated several times on different biofilms with the same qualitative observations: oxygen saturation increased significantly when an O_2 microsensor tip approached the biofilm and the perturbation affected a large area as compared to the size of the sensor tip (data not shown).
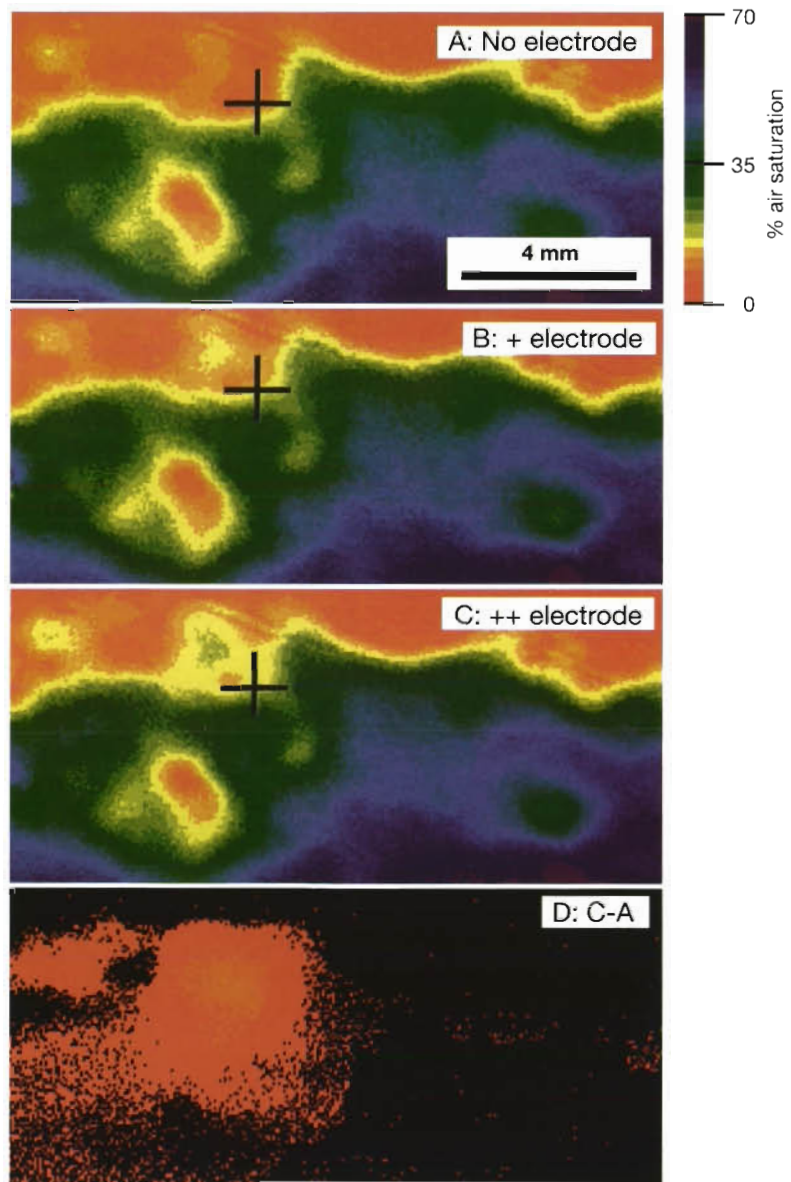

Fig. 7. Enlargement of the lower corner of the biofilm presented in Fig. 4 with a free flow velocity of 29.8 cm s^{-1}. Note that the scale bar is changed. (B) The tip of a microelectrode (+) was placed 200 µm above the surface of a biofilm and (C) 100 µm below the surface. (D) The O_2 images in (A) and (C) are subtracted and red pixels represents positions with an increased O_2 saturation after insertion of the microelectrode. A scale bar is included and the flow direction was from right to left

Organic carbon addition

Glucose was added to a final concentration of 2 mM in the water overlying the biofilm investigated in Fig. 4F, by injection into the reservoir (see Fig. 1A). The free flow velocity was kept at 35.1 cm s^{-1}. As new medium was continuously added at a rate of 50 ml min^{-1} the concentration of dissolved glucose gradually decreased. By washout the concentration of glucose decreased to <1 µM after 165 min. The addition of glucose resulted in an immediate decrease of the average O_2 saturation and a minimum value of 2.4% (7 µM) was reached after 11 min (Figs. 8 & 9). The O_2 saturation then stayed constantly low for another 15 min before it gradually increased to a constant level of approximately 11% air saturation (31 µM) after 160 min (Fig. 9). In another experiment acetate was removed from the usual medium during a steady state situation (flow velocity was 35.1 cm s^{-1}), but the O_2 saturation at the base of the 13 d old biofilm was unchanged even after 5 h without acetate (data not shown).

DISCUSSION

Flow related O_2 dynamics and the physical structure of biofilms

The presented data clearly demonstrate a complex and highly dynamic 2- and 3-dimensional O_2 distribution within a mature biofilm. Visual observations could to some extent relate the physical structure of the biofilms to the O_2 dynamics measured at the base. The investigated biofilms showed an extensive variation in thickness which was caused by dense cell clusters and channel structures, as has also been observed by others (e.g. Costerton et al. 1994). The location of these clusters and channels corresponded to low and high O_2 values, respectively. Despite the channel structures, well-developed biofilms with an average thickness >350 µm became completely anoxic at the base, at flow velocities below 6 cm s^{-1}, but at higher flow velocities, increased shear stress and pressure gradients gradually insured a better ventilation of the biofilms. Oxygen
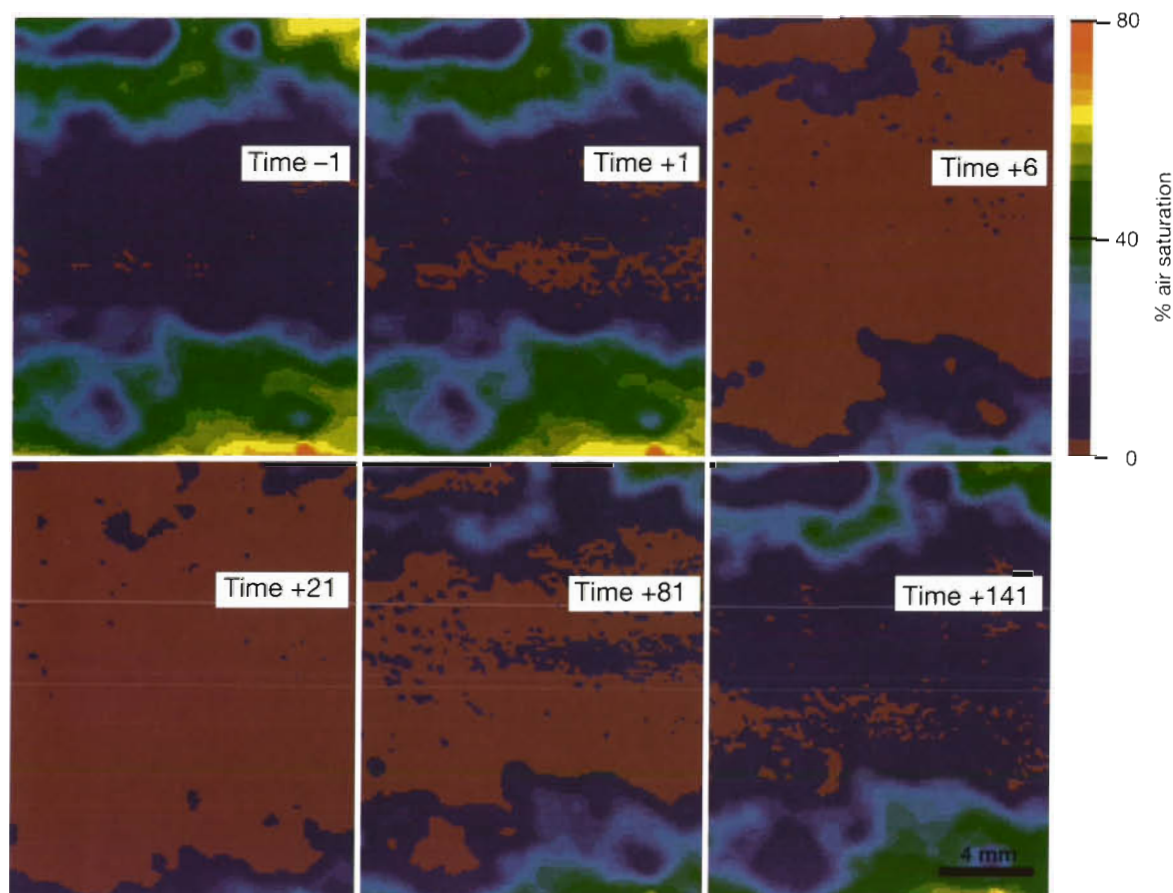

Fig. 8. Oxygen images of the base of a 13 d old biofilm at constant flow velocities before and after the addition of glucose to the free flowing water. Time is indicated in minutes and a positive sign indicates the time after glucose addition. The free flow velocity was 35.1 cm s^{-1} from right to left. A scale bar is shown in the last panel
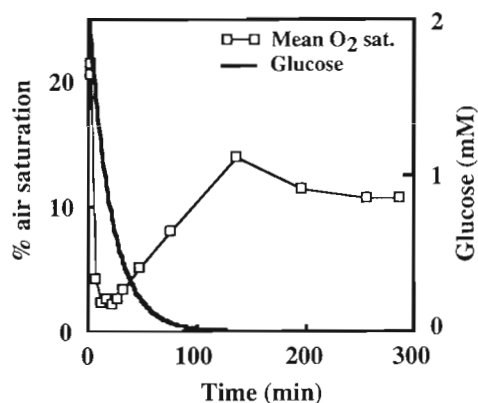
Fig. 9. Average O_2 saturation at the base of a 13 d old biofilm after the addition of glucose to a final concentration of 2 mM. The decrease in glucose concentration is solely estimated from the washout rate

images at higher flow velocities (e.g. Fig. 4) typically depicted areas with large densities of biomass and high O_2 consumptions in relatively O_2-rich surroundings. The base of the mature biofilms never reached full saturation, even at the base of the channels, indicating either a poor mixing between water in the channels and the overlying water or that the bottom of the channels was covered by a thin O_2-consuming community (base film). The development of the O_2-rich channels with increasing flow was incremental and typically a row of microoxic islands developed in otherwise anoxic surroundings and then fused into an O_2-rich channel. The fact that the O_2 channels were very flow sensitive and that reduced islands within channels exhibited step saturation gradients upstream and lower O_2 gradients downstream indicates that the channels contained flowing liquid (De Beer et al. 1996). Advective flow has been shown to occur in biofilms by a number of studies (e.g. Lewandowski et al. 1992, De Beer et al. 1994b). Increasing the flow above our maximum velocity would probably have further increased the O_2 saturation at the base (Fig. 5). However, at a certain point, resuspension and thereby disruption of the biofilm would have occurred.

The ventilation of different channels was not always linearly related to free flow velocity. It was often observed that as free flow velocity was incrementally increased the O_2 saturation in some channels was unaffected during some increments, while it increased significantly in others. These observations probably reflected the complex structure of a mature biofilm in which channels made up a complicated network with many intersection points. As the free flow velocity increased, interaction between changes in pressure gradients and shear stress in the different channels led to a complex enhancement of the biofilm ventilation. It was never observed that the O_2 saturation decreased at

any positions with increasing flow velocities, which would have indicated a physical change in the biofilm structure. In younger and less developed biofilm, the same observations were made. Here, however, the O_2 saturation at the base of clusters and channels was higher. At the highest flow velocities the O_2 saturation at the base of the these channels was close to 100%, especially when the channels were broad as in Fig. 2E.

Visual inspections showed that hairy structures on the surface of the biofilm moved or vibrated in the flow. The O_2 saturation at the base did not mimic these movements. The response time of the planar optodes was <1 s, indicating that these movements either did not cause fluctuations in the O_2 distribution at the base or that the fluctuation had a frequency faster than 1 Hz. However, even if movement of the hairy structures did not cause O_2 fluctuations at the base, it probably affected the steady state O_2 distribution within the biofilm.

Oxygen dynamics during development of a biofilm

The biofilms investigated here consisted of a very diverse population of bacteria and became established at a flow rate of approximately 20 cm s^{-1} on the surface of a planar optode coated with black silicone. The structure of biofilms varies but, in general, mature biofilms consist of cell clusters embedded in exopolymers that are separated by open voids (Costerton et al. 1994, Stewart et al. 1995). After reaching an average thickness of approximately 400 µm, the biofilm went into a stationary phase and the O_2 distribution at the base then remained stable for a period.

Unfortunately the frequent calibration that was required by our setup excluded the possibility of following the same section of the biofilm for a longer time. Construction of more stable planar optodes by integrating the experiences from microoptodes will probably overcome this problem (Klimant et al. 1995). Additionally, developments of fluorescence lifetime based techniques for planar optodes would improve the long-term stability and simplify the calibration procedures (Lippitsch et al. 1988).

Carbon limitation of a subpopulation of bacteria in the mature biofilms was illustrated by the immediate increase in O_2 consumption after addition of 2 mM glucose. The result was an extensive anoxia at the base of the biofilm even at maximum flow rate (Fig. 8). The anoxia rapidly expanded from the cell clusters, illustrating that O_2 was extracted from the water percolating the biofilm. The O_2 saturation in the overlying water was unchanged during this experiment, indicating that mixing between the overlying water and the water in the voids was too inefficient to supply electron

acceptors for the stimulated respiration. After 160 min, dilution had decreased the concentration of dissolved glucose to less than 1 µM. The new steady state O_2 saturation was significantly lower as compared to before glucose addition, probably due to retained glucose in the biofilm, allowing a higher specific respiration. This indicates a population of bacteria which presumably was living on non-optimal secondary metabolic compounds or on acetate as carbon source, but which could respire at a much higher rate on glucose. The omission of acetate from the medium had no effect on the O_2 distribution at the base of another mature biofilm investigated within a time horizon of 5 h. This shows that the acetate utilizing component of the biofilm contained an internal store of carbon which made respiration at the same rate possible for at least 5 h.

Flow and nutrient conditions typically fluctuate in nature and according to the acquired O_2 images this would have a significant impact on the O_2 conditions within a biofilm. Bacteria situated at a given position within a biofilm must experience a variety of oxic and anoxic conditions within relatively short time intervals. The presented data demonstrate the degree of metabolic flexibility which is required by bacteria living in such a dynamic structure.

Microsensor measurements in biofilms

The data presented in Fig. 7 demonstrate how the presence of a microsensor can change the oxic conditions within a biofilm. It has previously been shown that O_2 microsensors can compress the diffusive boundary layer and increase the O_2 saturations in coastal marine sediments (Glud et al. 1994). The mechanism behind this is not fully understood, but it is connected to local flow accelerations very close to the sensor tip (Glud et al. unpubl. data). The hydrodynamic changes induced by the presence of a sensor interact in 3 dimensions with the complex hydrodynamics at the biofilm water interface. The extent of the effect thus depends on the free flow velocity, the microsensor dimensions, and the 3-dimensional structure of the biofilm. The presented example was typical for the mature biofilms we investigated, but it was often observed that when the microsensor tip was placed in a channel between clusters, the disturbed area was more elongated, which again indicates liquid flow. It is clear that O_2 microsensor measurements in biofilms overestimate the O_2 penetration depth and the oxic conditions within a biofilm. In fact the investigated biofilm appeared totally oxic when measurements were carried out by microelectrodes, while the planar optode showed that the approximately 50% of the biofilm basis was anoxic. Since the effect is probably a func-

tion of sensor dimensions, great care has to be taken when microprofiles of different solutes, obtained by differently sized sensors, are aligned and interpreted. Likewise experiments with any intruding object, e.g. microinjection needles for flow studies, have to take the observed effects into account. Presumably the effects can be minimised by inserting sensors or needles from below so that the stem has no contact with the free flowing water (Glud et al. 1994). The disturbances introduced by microsensors illustrate the importance of local flow accelerations and microturbulences for solute distributions within biofilms. Extrusions or hairy structures typically observed in biofilms may indeed insure an efficient nutrient exchange several object diameters further downstream. Extensive microtopography may, in addition to channel structures, optimize the solute exchange between biofilm and overlying water through increased turbulence.

Application of the planar optodes techniques to biofilms has for the first time allowed the true O_2 distribution at the basis of biofilms to be resolved. Previously the oxic conditions at the basis were extrapolated from 1-dimensional approaches that by their presence changed the microenvironment. The extreme spatial and temporal variation in the aerobic conditions within biofilms has been demonstrated together with the large potential of planar optodes for studies of microenvironments in biofilms.

LITERATURE CITED

Caldwell DE, Korber DR, Lawrence JR (1992) Confocal laser microscopy and computer image analysis. Adv Microb Ecol 12:1–67

Canfield DE, Des Marais DJ (1993) Biogeochemical cycles of carbon, sulphur and free oxygen in a microbial mat. Geochim Cosmochim Acta 57:3971–3984

Costerton JW, Lewandowski Z, DeBeer D, Caldwell D, Korber D, James G (1994) Biofilms, the customized microniche. J Bacteriol 176:2137–2142

Dalsgaard T, Revsbech NP (1992) Regulating factors of denitrification in trickling filter biofilms as measured with oxygen/nitrous oxide microsensor. FEMS Microb Ecol 101: 151–164

DeBeer D, Stoodly P, Roe F, Lewandowski Z (1994a) Effects of biofilm structure on oxygen distribution and mass transport. Biotechnol Bioeng 43:1131–1138

DeBeer D, Stoodly P, Lewandowski Z (1994b) Liquid flow in heterogenous biofilms. Biotechnol Bioeng 44:636–641

DeBeer D, Stoodly P, Lewandowski Z (1996) Liquid flow and mass transport in heterogenous biofilms. Wat Res 30: 2761–2765

Ford T, Mitchell R (1991) The ecology of microbial corrosion. Adv Microb Ecol 11:231–262

Glud RN, Gundersen JK, Jørgensen BB, Revsbech NP (1994) Effects on the benthic diffusive boundary layer imposed by microelectrodes. Limnol Occanogr 39:462–467

Glud RN, Ramsing NB, Gundersen JK, Klimant I (1996) Planar optodes: a new tool for fine scale measurements of two-dimensional O_2 distribution in benthic communities. Mar Ecol Prog Ser 140:217–226

Glud RN, Ramsing NB, Revsbech NP (1992) Photosynthesis and photosynthesis coupled respiration in natural biofilms quantified with oxygen microsensors. J Phycol 28:51–60

Kautsky H (1939) Quenching of luminescence by oxygen. Trans Faraday Soc 35:216–219

Klimant I, Meyer V, Kühl M (1995) Fiber-optic oxygen micro-sensors, a new tool in aquatic biology. Limnol Oceanogr 40:1159–1165

Klimant I, Wolfbeis OS (1995) Oxygen sensitive luminescent materials based on silicone-soluble ruthenium diimine complexes. Anal Chem 34:3160–3166

Lawrence JR, Korber DR, Hoyle BD, Costerton JW, Caldwell DE (1991) Optical sectioning of microbial biofilms. J Bacteriol 173:6558–6567

Lewandowski Z, Altobelli DE, Majors PD, Fukushima E (1992) NMR imaging of hydrodynamics near microbially colonized surfaces. Wat Sci Technol 26:577–584

Lippitsch ME, Pusterhoffer J, Leiner MJP, Wolfbeis OS (1988) Fiber-optic oxygen sensor with the fluorescence decay time as the information carrier. Anal Chim Acta 205:16

Revsbech NP (1989) An oxygen microelectrode with a guard cathode. Limnol Oceanogr 34:474–478

Revsbech NP, Jørgensen BB (1986) Microelectrodes: their use in microbial ecology. Adv Microb Ecol 9:293–352

Stewart PS, Murga R, Srinivasan R, DeBeer D (1995) Biofilm structual heterogeneity visualized by three microscopic methods. Wat Res 29:2006–2009